Full Length
Arthritis & Rheumatology
DOI 10.1002/art.39948

Polymorphisms in the F pocket of HLA-B27 subtypes strongly impact on assembly, chaperone interactions and heavy chain misfolding

David B. Guiliano[1]* (PhD), Helen North[2]* (PhD), Eleni Panayoitou[3] (PhD), Elaine C. Campbell[4](PhD), Kirsty McHugh[5](PhD), Fiona G.M Cooke[4](BSc) , Marine Silvestre[4], Paul Bowness[5](MB BChir, DPhil), Simon J. Powis[4] (PhD) and Antony N. Antoniou[1,6] (PhD)

[1]David B. Guiliano and Antony N. Antoniou School of Health, Sport and Bioscience, University of East London, Stratford Campus, London E15 4LZ

[2]Helen Fussell, Histocompatibility and Immunogenetics Department, NHS Blood and Transplant, Colindale Blood Centre, Colindale Avenue, London, NW9 5BG

[3]Eleni Panayoitou, North West Surrey CCG, 58 Church Street, Weybridge, Surrey, KT13 8DP

[4]Simon J. Powis, Elaine C. Campbell, Fiona Cooke, Marine Silvestre, School of Medicine, University of St. Andrews, Fife, Scotland, KY16 9TF

[5]Kirsty McHugh, Paul Bowness, Nuffield Department of Orthopaedics Rheumatology and Musculoskeletal Science, Oxford, OX3 7LD

*These authors contributed equally to the work.

[6]Corresponding author: Antony N. Antoniou School of Health, Sport and Bioscience, University of East London, Stratford Campus, London E15 4LZ
Email: antoniouantony7@googlemail.com

Running Title: The impact of F pocket polymorphisms on HLA-B27 subtype folding

Funding: This work was in part funded by awards to Dr Antoniou (Arthritis Research UK Fellowship 15293) and Dr Powis (Scottish Government Chief Scientist Office ETM/56).

Conflicts of Interest: The authors have no conflicts to disclose.

Received: Feb 18, 2016; Revised: Aug 26, 2016; Accepted: Sep 29, 2016

Objective - HLA-B27 is associated with the inflammatory spondyloarthropathies (SpAs). Of significance, subtypes HLA-B*27:06 and HLA-B*27:09 are not associated with the SpAs. These subtypes primarily differ from the HLA-B*27:05 disease associated allele at residues 114 and 116 of the heavy chain, part of the F pocket of the antigen-binding groove. Dimerisation of HLA-B27 during assembly has been implicated in disease onset. This study investigated the factors influencing differences in dimerisation between disease associated and non-associated HLA-B27 alleles.

Methods – HLA-B*27:05 and mutants resembling the HLA-B*27:06 and 09 subtypes were expressed in the rat C58 T cell line, the human CEM T cell line and its calnexin deficient variant CEM.NKR. Immunoprecipitation, pulse chase, flow cytometry and immunoblotting were performed to study the assembly kinetics, heavy chain dimerisation and chaperone associations.

Results - By expressing HLA-B*27:05, 06-like and 09 alleles on a restrictive rat TAP peptide transporter background, we demonstrate that a tyrosine expressed at p116 or together with an aspartic acid residue at p114 inhibited HLA-B27 dimerisation and increased the assembly rate. F pocket residues alter the associations with chaperones of the early MHC class I folding pathway. Calnexin was demonstrated to participate in endoplasmic reticulum (ER) stress mediated degradation of dimers, whereas the oxidoreductase ERp57 does not appear to influence dimerization.

Conclusion - Residues within the F pocket of the peptide-binding groove differing between disease-associated and non-disease-associated HLA-B27 subtypes can influence the assembly process and heavy chain dimerisation, events which have been linked to the initiation of disease pathogenesis.

Human Leukocyte Antigen (HLA)-B27 is a major histocompatibility complex (MHC) class I molecule that exhibits a strong association with inflammatory arthritic conditions that are collectively referred to as the Spondyloarthropathies (SpAs) (1, 2). HLA-B27 exhibits an enhanced tendency to misfold and form aberrant dimeric structures (3, 4). HLA-B27 dimers were initially detected following recombinant protein purification and have subsequently been detected both *in vivo* in various cell lines (5-7) and in human patient derived cell types (8, 9). HLA-B27 dimer expression has also been correlated with disease incidence in the HLA-B27 rat transgenic model for Ankylosying Spondylitis (AS) (10). HLA-B27 heavy chain dimers were thought to form primarily via an unpaired cysteine (C) at position (p) 67 (7). Subsequently, we have demonstrated that HLA-B27 dimerisation inside cells can also involve the structurally conserved cysteines within the α2-domain of the heavy chain at p101 and p164 (6, 11).

Two HLA-B27 subtypes, HLA-B*27:06 and 09 exhibit no association with AS (12-14), though some contradictory data has previously been reported for HLA-B*27:09 (15, 16). These two subtypes have generated much interest due to their limited sequence differences compared to the canonical disease associated subtype HLA-B*27:05. HLA-B*27:09 possesses only an aspartic acid to histidine change at p116 (D116H), whilst the 06 subtype expresses an histidine to aspartic acid and an aspartic acid to tyrosine change at p114 and p116 respectively (termed 06-F pocket in this study) when compared to HLA-B*27:05. In addition HLA-B*27:06 expresses an aspartic acid to serine and valine to glutamate change at p77 and p152 respectively as well an alanine to glycine change at p211 within the α3 domain in comparison to HLA-B*27:05. The residues expressed by HLA-B*27:06 at p77 and p152 are shared with HLA-B*27:04, however 04 shares the same F pocket residues with HLA-B*27:05. Structurally, p114-116 constitute part of the F pocket of the peptide binding groove which binds and determines the carboxy (C) terminal motif of MHC class I associated peptides (17), but it can also influence other anchor positions (18). The 114-116 region also determines the ability of MHC class I molecules to use tapasin in optimising the peptide cargo and hence associate with the peptide-loading complex (PLC) during assembly in the ER (19). Thus the lack of association of the 06 and 09 subtypes with the SpA could support a role for either antigen presentation or protein folding participating in disease pathogenesis.

HLA-B27 dimerisation within the ER occurs early during MHC class I biosynthesis (5) and the maturation rate affects interactions between MHC class I heavy chains and pre-PLC associated chaperones (6). We have previously demonstrated that HLA-B*27:05, 06 and 09 subtypes differ in their cysteine accessibility to thiol-modifying drugs (6, 20) and recently characterised the ER stress associated degradation (ERAD) pathway of misfolded HLA-B27, involving the ERAD components EDEM1 and the E3 ubiquitin ligase HRD1 (8). We reasoned that if misfolding, particularly HC-dimerisation, is involved in disease pathogenesis, the HLA-B*27:06 and 09 subtypes should exhibit differences in their biochemical characteristics in comparison to HLA-B*27:05. We set out to test if 06 and 09 F pocket differences determine

which, if any, of the ER resident chaperones are involved in the dimerisation process and how these specific residues affect HLA-B27 folding. We demonstrate a role for calnexin in ER stress induced ERAD of HLA-B27 dimers, which is consistent with our proposed function for EDEM1 in dimer degradation (8). We also show a correlation between maturation rates and dimer formation, especially with F pocket residues expressed by the HLA-B*27:06 allele.

Materials and Methods

Cell lines and antibodies. The rat T cell line C58 (21) and the human T cell leukemia lines CEM and CEM.NKR were maintained in RPMI1640, supplemented with 10% FBS (Globepharm), penicillin, streptomycin and L-glutamine (R10 media) and maintained at 5% CO_2 and 37ºC. C58.B*27:05, H114D, HLA-B*27:09 (D116H), D116Y and 06 F Pocket (H114DD116Y), CEM.B*27:05, 06 F Pocket, HLA-A*02:01 and CEM.NKR.B*27:05, 06 F pocket and HLA-A*02:01 transfectants were generated by electroporation at 900 μF, 180 V and maintained in R10 media plus G418 (1 mg/ml). All constructs also included a V5 C-terminal tag. HEK 293 cells were maintained in R10 medium and transfected with shRNA targeted to ERp57 in the pSilencer 2.1 vector using Lipofectamine 2000 (both Life Technologies). Anti-V5 antibody (pK) was obtained from Serotec. Monoclonal antibody HC10 primarily recognises unfolded HLA-B and –C molecules. Anti-BiP and -CNX antibodies were obtained from Stressgen and anti-ERp57 from Abcam. Anti-BiP, -HERP and GAPDH antibodies were obtained from Santa Cruz Biotechnology. Goat anti-mouse HRP conjugated secondary antibody was obtained from DAKO and anti-rabbit monoclonal HRP from Sigma.

Site Directed Mutagenesis. For mutagenesis, a V5 C-terminally tagged cDNA encoding the HLA-B*27:05 allele, cloned into the mammalian expression vector pCR3.1 (Invitrogen) was mutated using PCR based site directed mutagenesis (Stratagene Quickchange) protocol as previously described (22).

Pulse Chase. Approx. 5 x 10^6 cells were preincubated in methionine free RPMI (Gibco), for 20 mins, labelled with 7.2 Mbq ^{35}S-Trans label (MP Biologicals) for 10 mins, washed and resuspended in R10 media. Aliquots were removed at specified times, lysed in 1% NP40 lysis buffer (150 mM NaCl, 10 mM Tris pH 7.4, 1 % NP40), supplemented with 1 mM PMSF, 1x complete protease inhibitors (Roche) and 10 mM NEM (Sigma). Samples were precleared for 30 mins with Protein A sepharose (Sigma) and immunoprecipitated with pK conjugated to 20 μl protein A sepharose for 1hr at 4ºC. Samples were resolved on 8% SDS-PAGE gels and processed for autoradiography.

Immunoprecipitation. Approx. 5 x 10^7 of each cell line were incubated with 20 mM NEM/PBS pH 6.8 on ice for 20 mins, followed by lysis in 1% NP40 lysis buffer. Lysates were precleared for 1hr at 4ºC, followed by immunoprecipitation with pK antibody (for MHC class I heavy chain immunoprecipitations) for 2 hrs at 4ºC. Immunoprecipitates were washed 5 x 0.5 mls with lysis buffer.

Immunoblotting. Samples were resolved on 8% SDS-PAGE, transferred onto nitrocellulose (BA85, Schleicher and Scheull), blocked for 1 hr with 5% skimmed milk powder in PBS/0.1% Tween, followed by overnight incubation with respective antibodies, followed by second stage HRP coupled antibodies. Images were revealed by chemiluminescence using Supersignal

Femto (Pierce). Images were developed on a BIORAD Fluoro-S Multimagere Max imager using Quantity One 1D analysis software.

Flow Cytometry. Approx 5 x 10^5 cells were incubated with ME1 or HC10 supernatant for 30 mins at 4°C, washed in PBS/1%FCS and incubated with FITC coupled anti-mouse antibodies for 30 mins, washed and fixed in 1% paraformaldehyde. Cells were analysed on a FACScalibur (Becton Dickinson).

qPCR quantitation. cDNA was generated using oligo dT primers and the Superscript™ III First Strand Synthesis kit (Invitrogen) according to manufacturer's conditions. Probes and primers specific for the spliced and unspliced mRNA transcripts for the human XBP-1 gene used sequence NM_005080 and for HLA-B*27:05 used the IMGT/HLA database (accession number HLA-00225, specific for HLA-B*27:05). Sequences were as follows; XBP-1 unspliced CACTCAGACTACGTGCACCTCTG (forward), XBP-1 spliced CTGAGTCCGCAGCAGGTG (forward), XBP-1 CAGAATCCATGGGGAGATGTT (reverse), XBP-1 CAGGCCCAGTTGTCACCCCTCCA (probe). For HLA-B*27:05, GACACAGATCTGCAAGGCCA (forward), TTGTAGTAGCGGAGCAGGGTC (reverse), CGCAGGTCCTCTCGGTCAGTCTGTG (probe). Probes and primers for the human ß-actin gene were obtained from Applied Biosystems (Part number 4333762T). 50 ng cDNA was tested in duplicate. Real time PCR was performed using conditions; 95ºC for 10 mins, 40 cycles of 95ºC for 15 secs and 64ºC for 1 min.

Results

Characterisation of cells expressing F pocket mutated HLA-B27 molecules. The locations of positions 114 and 116 in the F pocket, where the key polymorphisms between the HLA-B*27:05, 06 and 09 subtypes reside are shown in Figure 1A. We generated sets of C-terminal V5 tag HLA-B27 molecules with single residue substitutions found in different subtypes i.e. B27.H114D, B27.D116Y, B27.D116H (equivalent to the 09 subtype) or in combination i.e. B27.H114DD116Y (06-like, referred to hereafter as 06 F pocket) and expressed these in the rat thymoma C58 cell line. The C58 line has a *RT1*^{u} MHC background which is also shared with the PVG rat strain, which develops AS like disease in the presence of HLA-B27 (23, 24). The *RT1*^{U} TAP peptide transporter confers a more restrictive peptide transport profile than human TAP and is biased towards peptides with hydrophobic C-termini only (25). We reasoned that this more restricted TAP background might reveal factors influencing HLA-B27 assembly.

Analysis of cell surface expression of HLA-B*27:05 and the p114-116 subtype polymorphisms using the monoclonal antibodies ME1 (detecting folded HLA-B27) and HC10 (detecting partially unfolded HLA-B and –C molecules), indicated that residues expressed at p114-116 can alter cell surface expression in the *RT1*^{u} MHC background. The H114D substitution led to a reduction in cell surface expression (**Figure 1B**). HC10 expression overall mirrored those of ME1, Quantitative (q) PCR (data not shown) and protein expression analysis demonstrated, with the exception of HLA-B*27:09, all mutants were expressed within three fold of the HLA-B*27:05 subtype. In addition, this data indicates the reduced cell surface expression observed for H114D was not the result of a deficit of HLA-B27 heavy chain expression (**Figure 1C)**.

Residues at p114-116 influence the association with chaperones. It has been previously demonstrated that HLA-B*27:05 dimerisation occurs soon after translation (5) (and our unpublished observations) and F pocket residues can affect MHC class I assembly (26), therefore it is possible that ER resident chaperones associating with newly synthesized proteins may influence how these dimers are generated. The HLA-B27 heavy chain was immunoprecipitated, followed by immunoblotting for co-precipitating ER resident chaperones to determine which, if any of these residues influenced ER resident chaperone associations. Cells expressing HLA-B*27:05 and p114-116 substitutions were incubated with NEM to preserve transient disulfide bond interactions, lysed and immunoprecipitated through the anti-V5 epitope, resolved by non-reducing SDS-PAGE and immunoblotted for ERp57, calnexin (CNX), BiP, calreticulin (CRT) (data not shown), PDI (data not shown) and TPN (data not shown). HLA-B*27:05, H114D and HLA-B*27:09 formed conjugates with ERp57 and associated with CNX and BiP (**Figure 2**). The ERp57 immunoblot analysis also revealed several high molecular mass ERp57-MHC class I heavy chain conjugates (**Figure 2**, arrows b-f) as well as ERp57 monomers (**Figure 2**, arrow a). The ERp57-B27 conjugates were

different in size to HLA-B27 heavy chain dimers (data not shown). In contrast, there was lower association of these chaperones with the D116Y and 06 F pocket heavy chains. No association could be detected under these experimental conditions between HLA-B27 and PDI, CRT and TPN (data not shown), likely due to the use of NP40, which does not preserve most PLC interactions (27). Thus, F pocket differences amongst the HLA-B27 subtypes 05, 06 and 09 can influence associations with the chaperones CNX, BiP and the oxidoreductase ERp57 which can associate with newly synthesized proteins (28).

Calnexin and F pocket residues regulate HLA-B27 heavy chain dimer formation. CNX can control both the degradation and folding of substrate proteins including MHC class I molecules (29-31). We have previously shown that EDEM1 is involved in the ERAD of HLA-B27 dimers (8) with CNX integral to its function (32, 33). We therefore hypothesized that CNX may play a pivotal role in HLA-B27 dimerisation. To examine the role of CNX, we utilised the CNX deficient human cell line CEM.NKR. We transfected both the parental CNX expressing cell line CEM and CEM.NKR with HLA-B*27:05, 06 F Pocket, and as a control the non-disease associated MHC class I molecule HLA-A*02:01. The respective cell lines were NEM treated, lysed and proteins resolved by SDS-PAGE. Immunoblotting for MHC class I heavy chain revealed that HLA-B*27:05 produced dimer populations in CEM cells, whilst the control HLA-A*02:01 did not (**Figure 3A,** left panel). In NKR cells, HLA-B*27:05 displayed enhanced dimer formation (**Figure 3A,** middle panel). We could not detect dimers in either CEM or CEM.NKR cells expressing HLA-B*27:06 F pocket heavy chain (**Figure 3B,** right panel). Protein expression and qPCR analysis revealed that both CEM.B27 and NKR.B27 cell lines expressed similar levels of transfected HLA molecules (data not shown). The failure of HLA-A*02:01 to form dimer populations in normal or CNX deficient cell lines, indicates that the absence of CNX does not in itself cause the formation of HLA aggregates. These observations suggest CNX inhibits and/or reduces the formation of HLA-B27 dimers.

HLA-B27 can assemble in the absence of calnexin. The above data suggests that CNX regulates heavy chain dimers. We next studied the impact of CNX deficiency upon the expression and kinetics of HLA-B27 assembly. Cell surface expression of ME1 and HC10 reactive forms of HLA-B27 was determined. HLA-B*27:05 was similarly expressed by both CEM.B*27:05 and NKR.B*27:05 lines and as detected by ME1, whereas the HC10 staining was approximately two fold less in the absence of CNX (**Figure 3B & C**). Thus there are more partially folded or misfolded molecules at the cell surface in the presence of CNX. We next analysed the assembly kinetics by pulse chase analysis. HLA-B*27:05 displayed little acquisition of endo H resistance over 3 hrs chase, both in wild type or CNX deficient cells (**Figure 3D**). Over a longer time course endo H resistant material appeared at 3.5 hrs both in the wild type and calnexin deficient cells, with a slight increase in endo H resistant material evident in the presence of calnexin, quantified as 38% and 46% endo H resistant at 3.5 and 5

hours respectively in CEM cells, compared to 17% and 28% in NKR cells (**Figure 3E**). Thus the presence of CNX promoted faster assembly kinetics, but paradoxically this may result in less stable molecules which dissociate more readily at the cell surface.

HLA-B*27:05 heavy chain dimer detection is not dependent on ERp57 but ERAD is modulated by calnexin. CNX binds and recruits the oxidoreductase ERp57 (34) thus the absence of calnexin could potentially disrupt HLA-B*27:05 associations with ERp57, which may impact on dimerization. Therefore we immunoprecipitated MHC class I heavy chains from both CEM.B*27:05 and NKR.B*27:05 lines and immunoblotted for ERp57 associated with HLA-B27 (**Figure 4A**). ERp57 was associated with HLA-B*27:05 in both wild type and calnexin deficient cells. To determine if heavy chain dimerization was influenced by ERp57, we stably shRNA inhibited ERp57 in 293T cells (**Figure 4B**) followed by transient transfection with HLA-B*27:05. In the absence of ERp57, HLA-B27 retained the ability to dimerise (**Figure 4C**), however, minor alterations in the pattern of dimers were observed in ERp57 deficient cells, suggesting ERp57 may influence the composition of the dimerised pool.

Calnexin participates in degradation of misfolding polypeptide substrates in conjunction with the ER stress associated EDEM1 protein (33). We therefore examined if enhanced dimer levels were a result of reduced degradation in the absence of calnexin. CEM.B*27:05 and NKR.B*27:05 cells were therefore treated with tunicamycin, which induces ER stress induced ERAD responses (8). In the presence of calnexin, HLA-B27 dimers were absent following ER stress induction, however in the absence of calnexin, heavy chain dimers were retained (**Figure 4D**). To discount the possibility that calnexin deficient cells were unable to induce an ER stress response, we treated cells with tunicamycin or DTT and monitored the UPR activation markers BiP, the XBP-1 spliced (XBP-1s) transcription factor and the homocysteine-inducible ER stress protein (HERP) which is activated by XBP-1s. Pharmacological induction of ER stress led to enhanced BiP (2.9 and 5.4 fold increase in CEM and NKR respectively) and HERP (1.2 and 1.9 fold increase in CEM and NKR respectively) expression as detected by immunoblotting and enhanced XBP-1s transcript levels as determined by qPCR. Therefore in the absence of calnexin, the UPR can be induced (**Figure 4E & F**).

Residues at p114-116 alter dimerisation and maturation kinetics of HLA-B27. The above analysis demonstrated that F pocket residues can influence chaperone associations. We have previously hypothesized that the rate of maturation can correlate with dimer formation (6). We therefore examined how the F pocket residues influenced HLA-B27 dimerisation in rat C58 cells. D116Y had a reduced tendency to dimerise (**Figure 5A,** top panel), as did the 06 F pocket mutant (**Figure 5A,** bottom panel). After overnight incubation

at 26°C to slow the assembly kinetics, both the D116Y and 06 F pocket mutants displayed an ability to dimerise (**Figure 5A,** bottom panel), indicating there was no overall structural constraints preventing dimerisation.

Previously, we demonstrated that the ability of HLA-B27 to dimerise correlated with assembly kinetics (6), therefore we determined the effect that each of the F pocket residues had on the assembly kinetics of HLA-B27 (**Figure 5B**). HLA-B*27:05, B27.H114D, HLA-B*27:09, D116Y and 06 F pocket expressing cells were analysed by pulse chase. In this experiment we used an anti-V5 antibody directed at the C-terminus for the immunoprecipitation and were therefore able to detect all HLA-B27 molecules in an unbiased manner. Only a small proportion of the total HLA-B*27:05 and H114D molecules acquired endo H resistance (r) after 90 mins of chase, 3% and 0.5% respectively (**Figure 5B**), indicating that they remain within the ER for prolonged periods. However, residue changes at p116 dramatically changed maturation rates. HLA-B*27:09 (10% endo H resistant at 90 mins) has a markedly faster maturation rate than HLA-B*27:05, whilst the D116Y substitution was sufficient to further dramatically alter the maturation kinetics (29% at 90 mins). The 06 F pocket expressing HLA-B27 molecule exhibited an even faster maturation rate than the D116Y mutant (50% at 90 mins). Therefore, residues at p114-116 in the F pocket can have a dramatic impact on the maturation rate of HLA-B27.

Discussion.

The role that HLA-B27 plays in the pathogenesis of inflammatory arthritis remains elusive. Our data indicate that the residues at p114-116 dramatically affect the folding and dimer formation characteristics of HLA-B27 (summarised in cartoon form in **Figure 6**). Much of the focus regarding dimerisation has centered around C67, however our earlier observations and those of others suggested that C67 is not the sole cysteine responsible for dimerisation and that C164 may also participate in this process (6, 11). Previously, we demonstrated that p114-116 of HLA-B27 was also important in determining whether cysteine residues were exposed and reactive (20) (**Figure 6C-D**). The reduced tendency by D116Y and 06 F pocket mutant heavy chains to dimerise, may be related to the temporal exposure of reactive cysteines to the oxidizing environment of the ER (**Figure 6B**). Thus, together with the residues expressed at p114-116, the unpaired and structural cysteines proposed to be involved in dimerization may result in the ER resident population of heavy chain dimers being a complex mix of disulfide species involving multiple cysteine residues.

It has also been proposed that HLA-B27 dimers at the cell surface and within the cell may play a distinct role in disease pathogenesis (3, 35). ER resident dimers have been hypothesised to induce ER stress responses, possibly leading to proinflammatory cytokine production (35, 36). Cell surface dimers on the other hand lead to aberrant recognition by immune receptors (37, 38). In preliminary experiments with the HD6 antibody reagent that identifies cell surface HLA-B27 dimeric structures (39) we found no significant impact caused by the position 114 and 116 variants studied here, further supporting the idea that the cell surface HLA-B27 dimers are a distinct pool from the ER-resident forms (data not shown).

These current observations indicate that residues within the peptide-binding groove, representing polymorphisms found in HLA-B27 subtypes not associated with disease, play a critical role in determining the maturation rate of the molecule. Earlier work using conformationally specific antibodies ME1 and W6/32 (40, 41) corroborate our unbiased approach of monitoring HLA-B27 molecules expressing F pocket changes. These studies demonstrated that polymorphisms at p116 enhanced the acquisition of W6/32 and ME1 epitopes as well as affecting the ratio of folded vs HC10 reactive populations. Therefore, we suggest that the maturation rate of the HLA-B27 molecule influences whether cysteine residues are exposed to the oxidizing environment of the ER long enough to participate in aberrant disulfide bonding (**Figure 6B-D**).

The aspartic acid residue at p114 is expressed together with a tyrosine at p116 by HLA-B*27:06. However, the H114D mutation alone has a dramatic effect on cell surface expression levels of HLA-B27 compared to HLA-B*27:05 (**Figure 1B**), a finding consistent with previous observations (40). Interestingly, expression is restored to wild type levels at reduced temperatures ((40) and our unpublished observations), which indicates that there are

probably no gross primary structural alterations. Recently, biophysical and biochemical observations suggest that the HLA-B*27:05 and 04 peptide binding grooves exhibit greater degrees of flexibility and disorder when compared to HLA-B*27:06 and 09 (42, 43). It is possible that the cell surface expression levels that we observe in our peptide restricted environment, could be a reflection of the level of disorder within the HLA-B27 peptide-binding groove. The expression of tyrosine or histidine at p116 could reduce disorder (43), which may enhance peptide-binding stability, leading to improved folding dynamics and subsequently enhanced cell surface expression. However, the expression of aspartic acid at p114 in combination with an aspartic acid at p116 could increase the molecular disorder of the binding groove and disrupt the stability of peptide-MHC complexes.

Y116 appears to rescue or be dominant in its effect on HLA-B27 folding, which highlights that certain combinations of residues can influence MHC class I assembly (40, 44). Our observations highlight how the F pocket residues of HLA-B*27:06 affect the early stages of folding and dimerization. However, it would be of interest to determine any further effects of the HLA-B*27:06 serine and glutamate residues at p77 and p152 respectively. We can postulate that evolutionary pressure on MHC polymorphisms can select for combinations of residues, not only to enable the effective presentation of peptide, but also to allow for efficient folding and expression of MHC class I molecules. The above findings indicate that predicting the actual outcome of multiple mutations within the antigen binding groove on MHC class I molecules is difficult.

Intriguingly, the tyrosine at p116 is shared with HLA-B*27:07 which has been described as a subtype both associated and non-associated with AS. However, many studies suggest that HLA-B*27:07 exhibits a weaker association with AS (45, 46). Studies have demonstrated that HLA-B*27:07 and 06 can oligomerise to different extents (47). It remains undetermined how an asparagine at p114 in the absence of tyrosine and how the HLA-B*27:07 F pocket can affect the biochemical parameters we have described here. Our findings are consistent with previous observations that Y116 does enhance the maturation rate (44), but whether this is an important parameter in AS development remains undetermined. Our analysis does reveal differences in maturation rates and levels of dimerised HLA-B27 molecules. These observations could reflect differences between the rat C58 line with a restricted HLA-B27 binding peptide repertoire compared to human B and T lymphoblastoid lines such as CIR and 174.221.

HLA-B27 polymorphisms expressed at p114-116 can influence chaperone associations. These residues were thought to determine the requirement for tapasin within the PLC (19). In relation to HLA-B27, it has been described that polymorphisms expressed within the peptide binding groove by HLA-B27 subtypes influence thermostability (41, 48), F pocket flexibility (43) and requirement for tapasin (40). Here, we extend these studies to chaperones

associated with early folding events (**Figure 6**). It is possible that MHC class I heavy chain levels could influence chaperone associations. The higher expression levels of HLA-B*27:09 (**Figure 1**) could indeed account for BiP, calnexin and ERp57 co-precipitating with this molecule. D116Y and the 06 F pocket mutants, though expressed approximately 3 fold higher than HLA-B*27:05, only exhibit minimal levels if any at all of the co-precipitating chaperones (**Figure 2**). Previously, we have demonstrated that chaperone associations may depend on the MHC class I allele and rate of maturation. Incubation at reduced temperature can enhance chaperone associations (6). By reducing the temperature to 26°C, both D116Y and the 06 F pocket heavy chains can dimerise (**Figure 5**) and under these conditions, calnexin, BiP and ERp57 can be detected (our unpublished observations). These observations suggest that the folding and misfolding characteristics of MHC class I heavy chains are a predominant factor influencing chaperone association. Therefore, our data demonstrate that residues at p114 and 116 can influence associations with the oxidoreductase ERp57 and the chaperones, calnexin and BiP (**Figure 2**), which are involved in both early folding events of secretory proteins and their degradation (28, 49).

Our analysis of the role of ERp57 in HLA-B27 dimer formation in NKR.B27 cells indicates that this oxidoreductase does not require calnexin to associate directly with MHC class I heavy chains. We observed that ERp57 was found to form disulfide bonded conjugates with HLA-B27 heavy chains predisposed to forming dimeric conformations. However, ERp57 inhibition revealed that dimers could still be detected in the absence of ERp57. It is possible that dimerisation is a spontaneous event mediated by the oxidising conditions of the ER. However, HC-dimerisation could also be mediated by other oxidoreductases such as PDI. Dual inhibition of ERp57 and PDI in HLA-B27 expressing cells would address this question in the future.

Our data also supports a key role for calnexin in modulating dimer levels (**Figure 6A**). In the absence of calnexin, dimer levels are enhanced (**Figure 3).** Our analysis also reveals that calnexin can mediate degradation of dimers following the induction of ER stress (**Figure 4D**). This analysis is consistent with our previous observations demonstrating a role for EDEM1 in the degradation of HLA-B27 dimers (8). EDEM1 appears to require calnexin for efficient degradation of misfolding proteins (33) and EDEM1 is also a target for the ER stress inducible XBP-1s transcription factor (50). Therefore our observations are consistent with a role for calnexin and EDEM1 mediating dimer levels via an ER stress degradation pathway (**Figure 6A**).

Whilst the rat C58 cell line used in this study is unlikely to exactly represent the normal situation in human cells, due to its restricted TAP peptide transporter phenotype, it has allowed us to reveal key constraints imposed upon HLA-B27 assembly due to the residues at p114-116. The 06 and 09 subtypes share overlapping peptide repertoires with HLA-B*27:05

(51, 52). Situations where peptide supply might become a more limiting factor could arise in human cells such as those expressing some of the ERAP1 polymorphisms associated with AS (53). It has been suggested that ERAP1 polymorphisms do not affect ER stress in AS patients as determined by the expression of the early and late markers GRP78 and CHOP respectively (54). However, our previous observations suggest that there is an ER stress 'footprint' in AS derived patient samples, as determined by HRD1 expression (8). Thus, the detection of ER stress could be dependent on time and disease state, as well as the marker and cell type being analysed. Alternatively, if normal cellular homeostasis is disrupted, perhaps during viral or bacterial infections, or even just immune cell activation (55), this may also impose restrictions or alterations on peptide supply which then influences MHC class I peptide loading and maturation. Under these circumstances, heavy chain dimer formation could be enhanced and trigger an ERAD response to help clear the misfolded pool of heavy chains.

Our study demonstrates one of the first clear mechanistic links between subtype polymorphisms within the F pocket of the peptide-binding groove, disease incidence and the biochemical properties of these HLA-B27 molecules. Our observations highlight that F pocket residues can affect dimerization, chaperone association and alter the maturation rates of HLA-B27 subtypes. The pattern of dimerization and chaperone association correlates with HLA-B*27:06 and its non-association with AS, suggesting that these parameters may explain why HLA-B27:06 does not lead to an inflammatory situation. In addition, we have shown that ER stress induction can lead to calnexin-dependent dimer degradation and that exploiting the UPR induced ERAD pathway could well be a potential novel therapeutic approach.

References

1. Brewerton DA, Hart FD, Nicholls A, Caffrey M, James DC, Sturrock RD. Ankylosing spondylitis and HL-A 27. Lancet. 1973;1(7809):904-7.
2. Schlosstein L, Terasaki PI, Bluestone R, Pearson CM. High association of an HL-A antigen, W27, with ankylosing spondylitis. N Engl J Med. 1973;288(14):704-6.
3. Antoniou AN, Guiliano DB, Lenart I, Burn G, Powis SJ. The oxidative folding and misfolding of human leukocyte antigen-b27. Antioxid Redox Signal. 2011;15(3):669-84.
4. Bowness P. Hla-B27. Annu Rev Immunol. 2015;33:29-48.
5. Dangoria NS, DeLay ML, Kingsbury DJ, Mear JP, Uchanska-Ziegler B, Ziegler A, et al. HLA-B27 misfolding is associated with aberrant intermolecular disulfide bond formation (dimerization) in the endoplasmic reticulum. The Journal of Biological Chemistry. 2002;277(26):23459-68.
6. Antoniou AN, Ford S, Taurog JD, Butcher GW, Powis SJ. Formation of HLA-B27 homodimers and their relationship to assembly kinetics. The Journal of Biological Chemistry. 2004;279(10):8895-902.
7. Allen RL, O'Callaghan CA, McMichael A, Bowness P. HLA-B27 forms a novel heavy chain homodimer structure. Journal of Immunology. 1999;162:5045-8.
8. Guiliano DB, Fussell H, Lenart I, Tsao E, Nesbeth D, Fletcher AJ, et al. Endoplasmic reticulum degradation-enhancing alpha-mannosidase-like protein 1 targets misfolded HLA-B27 dimers for endoplasmic reticulum-associated degradation. Arthritis & Rheumatology. 2014;66(11):2976-88.
9. Campbell EC, Fettke F, Bhat S, Morley KD, Powis SJ. Expression of MHC class I dimers and ERAP1 in an ankylosing spondylitis patient cohort. Immunology. 2011;133(3):379-85.
10. Tran TM, Satumtira N, Dorris ML, May E, Wang A, Furuta E, et al. HLA-B27 in transgenic rats forms disulfide-linked heavy chain oligomers and multimers that bind to the chaperone BiP. Journal of Immunology. 2004;172(8):5110-9.
11. Lenart I, Guiliano DB, Burn G, Campbell EC, Morley KD, Fussell H, et al. The MHC Class I Heavy Chain Structurally Conserved Cysteines 101 and 164 Participate in HLA-B27 Dimer Formation. Antioxid Redox Signal. 2011;16(1):33-43.
12. Ramos M, Lopez de Castro JA. HLA-B27 and the pathogenesis of spondyloarthritis. Tissue Antigens. 2002;60(3):191-205.
13. Khan MA. Polymorphism of HLA-B27: 105 subtypes currently known. Curr Rheumatol Rep. 2013;15(10):362.
14. Taurog JD, Chhabra A, Colbert RA. Ankylosing Spondylitis and Axial Spondyloarthritis. N Engl J Med. 2016;374(26):2563-74.
15. Olivieri I, D'Angelo S, Scarano E, Santospirito V, Padula A. The HLA-B*2709 subtype in a woman with early ankylosing spondylitis. Arthritis and Rheumatism. 2007;56(8):2805-7.
16. Cauli A, Vacca A, Mameli A, Passiu G, Fiorillo MT, Sorrentino R, et al. A Sardinian patient with ankylosing spondylitis and HLA-B*2709 co-occurring with HLA-B*1403. Arthritis and Rheumatism. 2007;56(8):2807-9.
17. Falk K, Rotzschke O, Stevanovic S, Jung G, Rammensee HG. Allele-specific motifs revealed by sequencing of self-peptides eluted from MHC molecules. Nature. 1991;351(6324):290-6.
18. Sesma L, Montserrat V, Lamas JR, Marina A, Vazquez J, Lopez de Castro JA. The peptide repertoires of HLA-B27 subtypes differentially associated to spondyloarthropathy (B*2704 and B*2706) differ by specific changes at three anchor positions. The Journal of Biological Chemistry. 2002;277(19):16744-9.
19. Williams AP, Peh CA, Purcell AW, McCluskey J, Elliott T. Optimization of the MHC class I peptide cargo is dependent on tapasin. Immunity. 2002;16(4):509-20.
20. Fussell H, Nesbeth D, Lenart I, Campbell EC, Lynch S, Santos S, et al. Novel detection of in vivo HLA-B27 conformations correlates with ankylosing spondylitis association. Arthritis and Rheumatism. 2008;58(11):3419-24.
21. Silva A, MacDonald HR, Conzelmann A, Corthesy P, Nabholz M. Rat X mouse T-cell hybrids with inducible specific cytolytic activity. Immunological Reviews. 1983;76:105-29.
22. Antoniou AN, Ford S, Alphey M, Osborne A, Elliott T, Powis SJ. The oxidoreductase ERp57 efficiently reduces partially folded in preference to fully folded MHC class I molecules. The EMBO Journal. 2002;21(11):2655-63.

23. Utriainen L, Firmin D, Wright P, Cerovic V, Breban M, McInnes I, et al. Expression of HLA-B27 causes loss of migratory dendritic cells in a rat model of spondylarthritis. Arthritis and Rheumatism. 2012;64(10):3199-209.
24. Taurog JD, Maika SD, Satumtira N, Dorris ML, McLean IL, Yanagisawa H, et al. Inflammatory disease in HLA-B27 transgenic rats. Immunological Reviews. 1999;169:209-23.
25. Momburg F, Roelse J, Howard JC, Butcher GW, Hammerling GJ, Neefjes JJ. Selectivity of MHC-encoded peptide transporters from human, mouse and rat. Nature. 1994;367(6464):648-51.
26. Neefjes JJ, Ploegh HL. Allele and locus-specific differences in cell surface expression and the association of HLA class I heavy chain with beta 2-microglobulin: differential effects of inhibition of glycosylation on class I subunit association. European Journal of Immunology. 1988;18(5):801-10.
27. Cresswell P, Bangia N, Dick T, Diedrich G. The nature of the MHC class I peptide loading complex. Immunological reviews. 1999;172:21-8.
28. Antoniou AN, Powis SJ, Elliott T. Assembly and export of MHC class I peptide ligands. Current Opinion in Immunology. 2003;15(1):75-81.
29. Lederkremer GZ. Glycoprotein folding, quality control and ER-associated degradation. Curr Opin Struct Biol. 2009;19(5):515-23.
30. Maattanen P, Gehring K, Bergeron JJ, Thomas DY. Protein quality control in the ER: the recognition of misfolded proteins. Semin Cell Dev Biol. 2010;21(5):500-11.
31. Vassilakos A, Cohen-Doyle MF, Peterson PA, Jackson MR, Williams DB. The molecular chaperone calnexin facilitates folding and assembly of class I histocompatibility molecules. The EMBO Journal. 1996;15(7):1495-506.
32. Oda Y, Hosokawa N, Wada I, Nagata K. EDEM as an acceptor of terminally misfolded glycoproteins released from calnexin. Science. 2003;299(5611):1394-7.
33. Molinari M, Calanca V, Galli C, Lucca P, Paganetti P. Role of EDEM in the release of misfolded glycoproteins from the calnexin cycle. Science. 2003;299(5611):1397-400.
34. Pollock S, Kozlov G, Pelletier MF, Trempe JF, Jansen G, Sitnikov D, et al. Specific interaction of ERp57 and calnexin determined by NMR spectroscopy and an ER two-hybrid system. The EMBO Journal. 2004;23(5):1020-9.
35. Antoniou AN, Lenart I, Guiliano DB. Pathogenicity of Misfolded and Dimeric HLA-B27 Molecules. Int J Rheumatol. 2011;2011:486856.
36. Colbert RA. HLA-B27 misfolding: a solution to the spondyloarthropathy conundrum? [In Process Citation]. Mol Med Today. 2000;6(6):224-30.
37. Bird LA, Peh CA, Kollnberger S, Elliott T, McMichael AJ, Bowness P. Lymphoblastoid cells express HLA-B27 homodimers both intracellularly and at the cell surface following endosomal recycling. European Journal of Immunology. 2003;33(3):748-59.
38. Kollnberger S, Bird L, Sun MY, Retiere C, Braud VM, McMichael A, et al. Cell-surface expression and immune receptor recognition of HLA-B27 homodimers. Arthritis and Rheumatism. 2002;46(11):2972-82.
39. McHugh K, Rysnik O, Kollnberger S, Shaw J, Utriainen L, Al-Mossawi MH, et al. Expression of aberrant HLA-B27 molecules is dependent on B27 dosage and peptide supply. Annals of the Rheumatic Diseases. 2014;73(4):763-70.
40. Goodall JC, Ellis L, Hill Gaston JS. Spondylarthritis-associated and non-spondylarthritis-associated B27 subtypes differ in their dependence upon tapasin for surface expression and their incorporation into the peptide loading complex. Arthritis and Rheumatism. 2006;54(1):138-47.
41. Galocha B, Lopez de Castro JA. Mutational analysis reveals a complex interplay of peptide binding and multiple biological features of HLA-B27. The Journal of Biological cChemistry. 2010;285(50):39180-90.
42. Loll B, Fabian H, Huser H, Hee CS, Ziegler A, Uchanska-Ziegler B, et al. Increased Conformational Flexibility of HLA-B*27 Subtypes Associated With Ankylosing Spondylitis. Arthritis & Rheumatology. 2016;68(5):1172-82.
43. Abualrous ET, Fritzsche S, Hein Z, Al-Balushi MS, Reinink P, Boyle LH, et al. F pocket flexibility influences the tapasin dependence of two differentially disease-associated MHC Class I proteins. European Journal of Immunology. 2015;45(4):1248-57.
44. Galocha B, de Castro JA. Folding of HLA-B27 subtypes is determined by the global effect of polymorphic residues and shows incomplete correspondence to ankylosing spondylitis. Arthritis and Rheumatism. 2008;58(2):401-12.

45. Varnavidou-Nicolaidou A, Karpasitou K, Georgiou D, Stylianou G, Kokkofitou A, Michalis C, et al. HLA-B27 in the Greek Cypriot population: distribution of subtypes in patients with ankylosing spondylitis and other HLA-B27-related diseases. The possible protective role of B*2707. Human Immunology. 2004;65(12):1451-4.
46. Gomez P, Montserrat V, Marcilla M, Paradela A, de Castro JA. B*2707 differs in peptide specificity from B*2705 and B*2704 as much as from HLA-B27 subtypes not associated to spondyloarthritis. European Journal of Immunology. 2006;36(7):1867-81.
47. Jeanty C, Sourisce A, Noteuil A, Jah N, Wielgosik A, Fert I, et al. HLA-B27 subtype oligomerization and intracellular accumulation patterns correlate with predisposition to spondyloarthritis. Arthritis & Rheumatology. 2014;66(8):2113-23.
48. Hillig RC, Hulsmeyer M, Saenger W, Welfle K, Misselwitz R, Welfle H, et al. Thermodynamic and structural analysis of peptide- and allele-dependent properties of two HLA-B27 subtypes exhibiting differential disease association. The Journal of Biological Chemistry. 2004;279(1):652-63.
49. Hebert DN, Molinari M. In and out of the ER: protein folding, quality control, degradation, and related human diseases. Physiol Rev. 2007;87(4):1377-408.
50. Lee AH, Iwakoshi NN, Glimcher LH. XBP-1 regulates a subset of endoplasmic reticulum resident chaperone genes in the unfolded protein response. Molecular and Cellular Biology. 2003;23(21):7448-59.
51. Garcia F, Marina A, Lopez de Castro JA. Lack of carboxyl-terminal tyrosine distinguishes the B*2706-bound peptide repertoire from those of B*2704 and other HLA-B27 subtypes associated with ankylosing spondylitis. Tissue Antigens. 1997;49(3 Pt 1):215-21.
52. Garcia-Peydro M, Marti M, Lopez de Castro JA. High T cell epitope sharing between two HLA-B27 subtypes (B*2705 and B*2709) differentially associated to ankylosing spondylitis. Journal of Immunology. 1999;163(4):2299-305.
53. Reeves E, Colebatch-Bourn A, Elliott T, Edwards CJ, James E. Functionally distinct ERAP1 allotype combinations distinguish individuals with Ankylosing Spondylitis. Proc Natl Acad Sci U S A. 2014;111(49):17594-9.
54. Kenna TJ, Lau MC, Keith P, Ciccia F, Costello ME, Bradbury L, et al. Disease-associated polymorphisms in ERAP1 do not alter endoplasmic reticulum stress in patients with ankylosing spondylitis. Genes and Immunity. 2015;16(1):35-42.
55. Santos SG, Lynch S, Campbell EC, Antoniou AN, Powis SJ. Induction of HLA-B27 heavy chain homodimer formation after activation in dendritic cells. Arthritis Research & Therapy. 2008;10(4):R100.

Figure Legends

Figure 1. Illustration of p114 and p116 residues within the HLA-B27 antigen binding groove and expression of the p114-116 F pocket HLA-B27 molecules in the rat thymoma C58 cell line. (**A**) iCn3D generated images of the HLA-B*27:05 antigen binding groove, using structure 1HSA. Position 114 is indicated in blue, position 116 is indicated in green. (**B**) HLA-B*27:05, H114D, HLA-B*27:09, D116Y and 06 F pocket molecule expression at the cell surface of C58 rat thymoma cells. The aforementioned cell lines and the untransfected (UT) C58 cell line were analysed by flow cytometry with antibodies ME1 and HC10. (**C**) Protein quantitation of F pocket mutants relative to HLA-B*27:05. C58 cell lines expressing HLA-B*27:05, the HLA-B27 F pocket mutants and untransfected C58 cell line were lysed and equivalent concentration of protein resolved by non-reducing SDS-PAGE. Lysates were immunoblotted for MHC class I heavy chain and expression.

Figure 2. Residues 114-116 of HLA-B27 alter ER chaperone associations. Untransfected C58 cells and those expressing HLA-B*27:05 and subtype polymorphisms H114D, HLA-B*27:09, D116Y, and the 06 F pocket were immunoprecipitated through the V5 tag and immunoblotted for ERp57, calnexin and BiP. Immunoblotting detected ERp57 disulfide conjugates with HLA-B*27:05, H114D and D116H as well as ERp57 monomer. Immunoblotting detected calnexin and BiP co-precipitating with HLA-B*27:05, H114D and HLA-B*27:09. Arrow a; monomeric ERp57, arrow b-f; HLA-B27-ERp57 disulfide bonded conjugates. Reduced lysates from the above cell lines were resolved by SDS-PAGE and immunoblotted with ERp57, calnexin and BiP illustrating equal loading. Reduced lysates were also probed for HLA-B27 heavy chain using the V5 tag and immunoblot analysis indicates approximately equal levels of MHC class I heavy chain except for HLA-B*27:09. One of four independent experiments is shown.

Figure 3. Calnexin and 06 F pocket residues modulate levels of HLA-B27 heavy chain dimers, and the absence of calnexin does not significantly perturb folding kinetics of HLA-B27 (**A)** HLA-B*27:05, HLA-A*02:01 and 06 F pocket were expressed in CEM and CEM.NKR cells. Immunoblotting for MHC class I heavy chain revealed enhanced levels of B27 dimers (arrows 1, 2 and 3) in NKR.HLA-B27 cells compared to CEM.B27. HLA-A*02:01 and 06 F pocket did not form dimers. (B) CEM.B27 and (C) NKR.B27 cells were analysed by flow cytometry. ME1 and HC10 reactive molecules were detected. Mean fluorescence intensities (MFI) figures for CEM.B27 were 2^{o}:75, HC10:283 and ME1:2192. MFI figures for NKR.B27 were 2^{o}:85, HC10:174 and ME1:1851. (**D and E**) CEM.B27 and NKR.B27 cell lines were metabolically labeled for 15 mins and chased for the indicated times. Lysates were immunoprecipitated with the anti-V5 tag antibody, incubated with endo H and resolved by reducing SDS-PAGE (one of three experiments shown).

Figure 4. ERp57 does not influence heavy chain dimer formation, whilst calnexin modulates dimer degradation via ER stress induced ERAD. (**A**) CEM, CEM.B*27:05, NKR and NKR.B*27:05 cells were immunoprecipitated for HLA-B27 with the V5 tag antibody and immunoblotted for ERp57. HLA-B27-ERp57 conjugates were detected in the CEM.B27 and NKR.B27 cell lines. (**B**) Stable ERp57 shRNA knockdown 293T cell lysates were immunoblotted for ERp57, PDI, ERp72, calreticulin (CRT) and CNX. (**C**) 293T wt and ERp57 knockdowns were transiently transfected with HLA-B*27:05. Lysates were probed for MHC class I heavy chain using the HC10 antibody. (**D**) Degradation of HC-dimers via UPR induced ERAD in the presence but not in the absence of calnexin. CEM.B27 and NKR.B27 cells were treated with tunicamycin (TUN), and lysates immunoblotted for HLA-B27 using the V5 antibody. Mock (M) treated cells were incubated with DMSO alone, untreated cells (0) (**E**) Induction of the UPR in the presence and absence of calnexin. CEM and NKR cells were incubated with 5 mM DTT, RNA extracted and qRT-PCR of the XBP-1 spliced product was determined. (**F**) CEM and NKR cells were treated with TUN and lysates were immunoblotted for BiP, HERP and GAPDH.

Figure 5. F pocket p114-116 residues alter the ability of HLA-B27 to mature and dimerise. (**A**) Lysates from C58 cells expressing HLA-B*27:05, HLA-B*27:09, D116Y, H114D and HLA-A*02:01 were resolved by non-reducing SDS-PAGE and immunoblotted for the V5 tag. The D116Y substitution exhibits a reduced tendency to dimerise (top panel). C58 cells expressing D116Y and 06 F pocket were incubated overnight at 37°C or 26°C. Lysates were then resolved by non-reducing SDS-PAGE and immunoblotted for the V5 tag. D116Y and 06 F pocket exhibit a reduced tendency to dimerise at 37°C, whilst both can dimerise following incubation at reduced temperature (bottom panel). (**B**) C58 cells with p114-116 polymorphisms were analysed by flow cytometry with antibodies ME1, HC10 and HD6. Shaded histograms represent staining of untreated cells and unshaded histograms represent staining following acid treatment. (**C**) Pulse-chase analysis of HLA-B*27:05 and subtype polymorphisms H114D, HLA-B*27:09, D116Y and 06 F pocket (r - endo H resistant, s – endo H sensitive). Cell lines were metabolically labeled, chased for 0, 45 and 90 mins, immunoprecipitated with the anti-V5 antibody and resolved by reducing SDS-PAGE. HLA-B*27:09, D116Y and 06 F pocket exhibit more rapid acquisition of endo H resistance (one of three experiments shown).

Figure 6. Schematic showing the folding pathways of HLA-B27 and outcomes of ER resident HC-dimerisation. (**A**) Newly synthesized HLA-B*27:05 heavy chains translocated via the sec61 complex, strongly associate with calnexin (CNX)-ERp57 as well as the Immunoglobulin Binding Protein (BiP) (6, 10, 28). The relationship between heavy chains associated with BiP and CNX-ERp57 remains undefined (denoted by '?'). Following the non-covalent association with the light chain beta-2-microglobulin (β2m) CNX is displaced. HLA-B27 can acquire an optimal peptide cargo through the association with the peptide loading complex (PLC), whose

predominant constituents are the Transporter Associated with antigen Presentation (TAP), tapasin (TPN), calreticulin (CRT) and ERp57 (19, 28). HLA-B27 can transit to the cell surface independently of the PLC. HLA-B*27:05 can also form HC-dimers, which potentially can activate the Unfolded Protein Response (UPR) (11). The UPR induced transcription factor XBP-1 can target genes with a UPRE promoter sequence (50). EDEM1 and HRD1 can be activated by XBP-1 and together with SEL1 form an ER stress induced protein degradation complex (8). Through the action of CNX, HC-dimers can be targeted for destruction via the ER stress induced degradation complex. (**B**) 06 F pocket and D116Y residues result in transient associations with the chaperones CNX-ERp57 and BiP. Both exhibit a fast maturation rate (30-45 mins) of folded HLA class I molecules (40), resulting in little if any formation of HC-dimers. (**C**) HLA-B*27:09 exhibits a slower maturation rate (90 mins), which can result in the formation of both folded and dimeric conformers. (**D**) HLA-B*27:05 and H114D exhibit exposed and reactive cysteines (depicted by□□) to a greater extent than HLA-B*27:09 (depicted in C by □) (20). Both these molecules have an enhanced tendency to misfold and form HC-dimers, whilst exhibiting prolonged associations with CNX-ERp57 and BiP. HLA-B*27:05 molecules transit through the ER at a slow rate (3.5 hrs). For B-D, times in mins or hours are maturation rates of HLA-B27 heavy chains as determined by acquisition of endo H resistance.

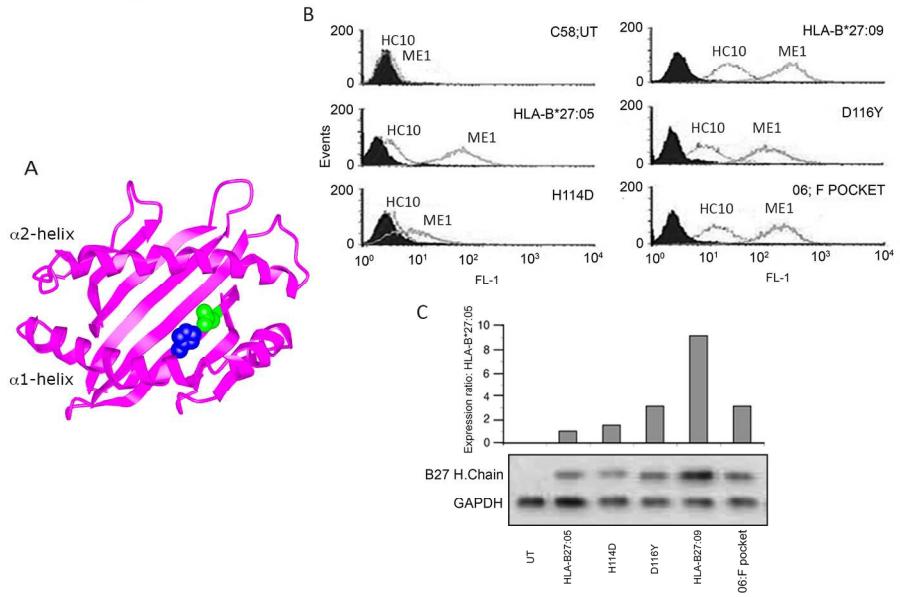

Figure 1

177x114mm (300 x 300 DPI)

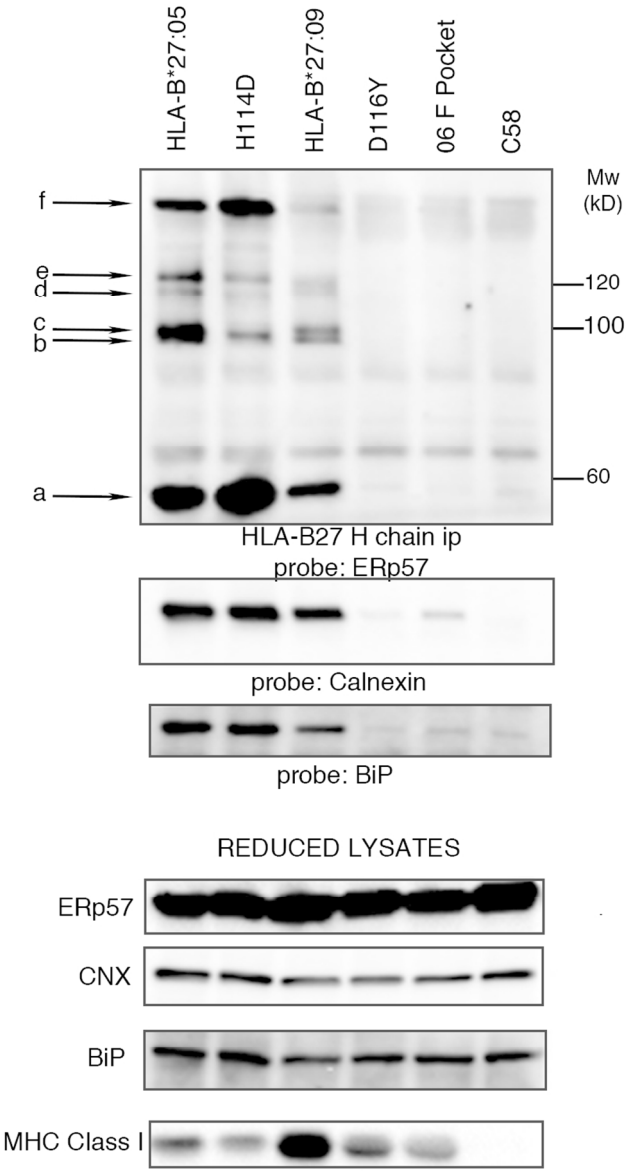

Figure 2

69x130mm (300 x 300 DPI)

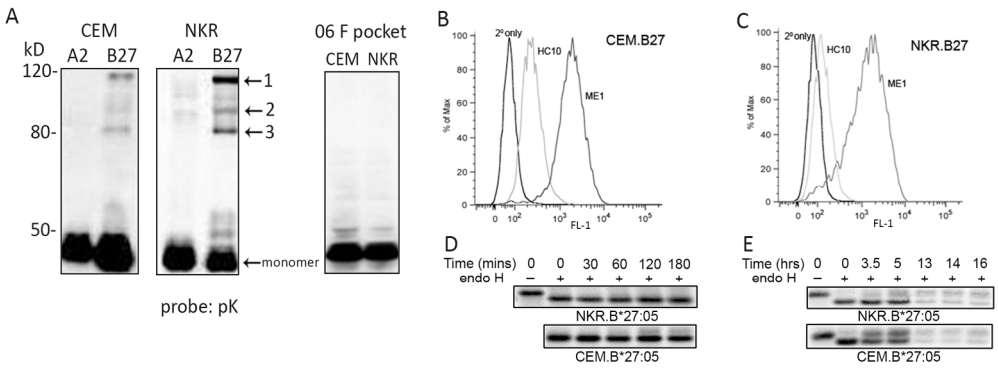

Figure 3

176x67mm (300 x 300 DPI)

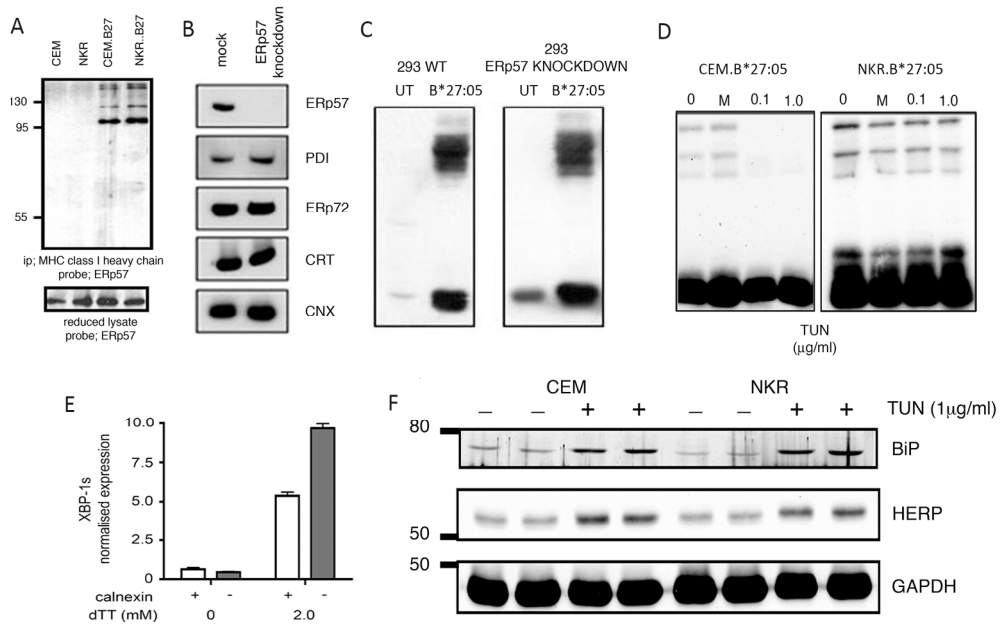

Figure 4

173x108mm (300 x 300 DPI)

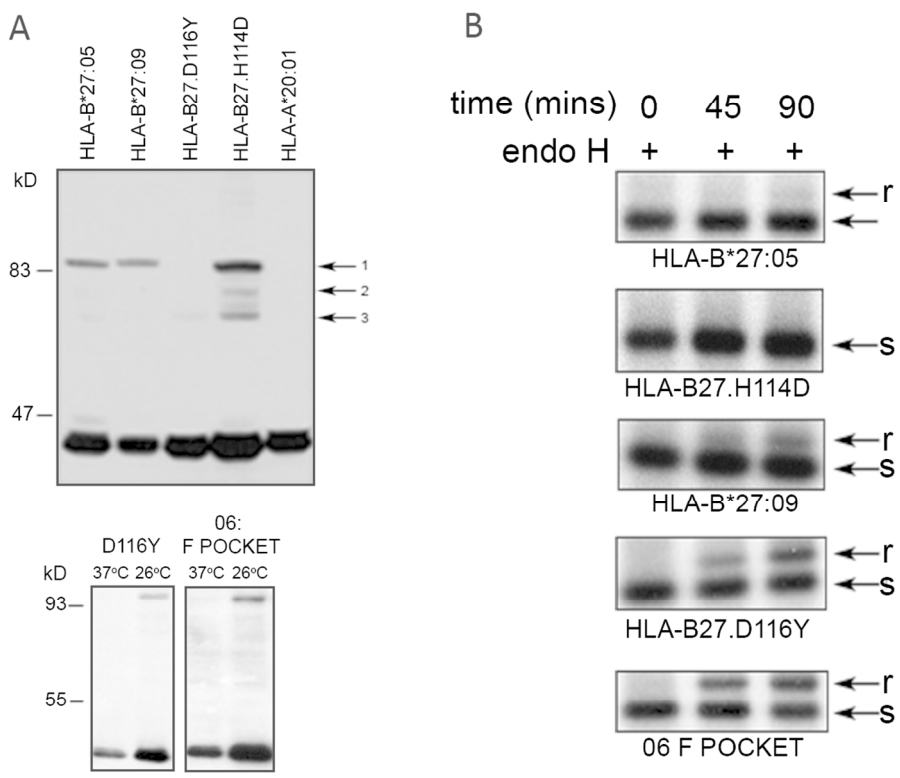

Figure 5

111x88mm (300 x 300 DPI)

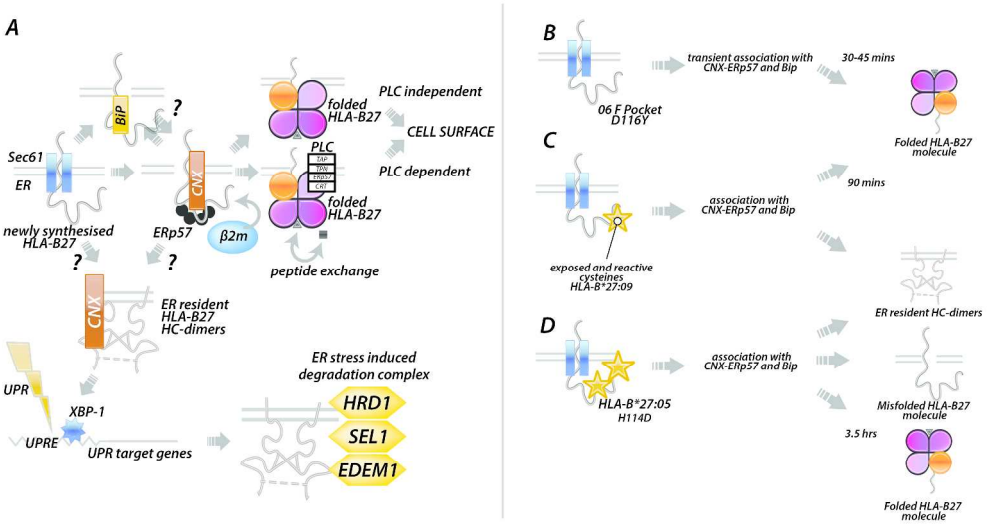

Figure 6

363x207mm (300 x 300 DPI)